

Resonant Production of Color Octet Muons at the Future Circular Collider Based Muon-Proton Colliders^{*}

Y. C. Acar¹⁾ U. Kaya^{1,2)} B. B. Oner¹⁾

¹⁾ Department of Material Science and Nanotechnology, TOBB University of Economics and Technology, Ankara 06560, Turkey

²⁾ Department of Physics, Ankara University, Ankara 06560, Turkey

Abstract: We investigate the resonant production of color octet muons in order to explore the discovery potential of the FCC-based μp colliders. It is shown that search potential of μp colliders essentially surpass the potential of the LHC and would exceed that of the FCC pp collider.

Key words: leptogluons, lepton-hadron interactions, composite models, muon-proton colliders, color octet muon, beyond the standard model

1 Introduction

High energy physics experiments performed in recent decades show that Standard Model (SM) is consistent in a low energy regime. However, there are still phenomenological and theoretical problems and questions to be answered. Experimental research for the new physics, searching for these answers for higher energies, relies on recently developed accelerator technologies. Energy frontier lepton colliders seem to be prominent candidates to investigate the validity of the SM at high energies, and they have the potential to reveal novelties that lie beyond the Standard Model (BSM). Producing and colliding muon beams with intense bunches to achieve sufficiently high luminosities is still a promising topic. In this regard, a recent paper by the Muon Accelerator Program (MAP) addressed designs of various center of mass (CM) energy muon colliders (μC) from 126 GeV (Higgs-factory) to multi-TeV (energy frontier) options [1]. Also ultimate case muon colliders with CM energy up to 100 TeV were considered in another study, and parameters of these colliders were given [2].

Developing the technology of lepton colliders makes high luminosity and high CM energy lepton-hadron colliders possible. In this manner, one can utilize the advantages of their vital role in understanding the fundamental structure of matter using the highest energy hadron beams, which will be provided by the Future Circular Collider (FCC) [3]. In the near future, it is expected that the construction of μp machines can also be considered, depending on the solutions to the principal issues of

the $\mu^+\mu^-$ colliders. Some advantages of the highest energy μp machines can be listed briefly as follows. Firstly, multi-TeV scale muon-proton collisions are testing mechanisms of composite models and may give us clear hints about the fermion mixing and generation replication puzzle of the SM fermions. In addition, they would present experimental results that enable us to understand the QCD better. Exotic particle productions are more probable compared to the ep colliders since the large mass ratio between muon and electron [4].

Muon-proton colliders were proposed two decades ago. Construction of additional proton ring in $\sqrt{s}=4$ TeV muon collider tunnel was suggested in [4] to handle μp collider with the same CM energy. However, luminosity value, namely $L_{\mu p} = 3 \times 10^{35} \text{cm}^{-2} \text{s}^{-1}$, was extremely overestimated, a realistic value for this should be three orders smaller [5]. Then, construction of additional 200 GeV energy muon ring in the Tevatron tunnel in order to handle $\sqrt{s} = 0.9$ TeV μp collider with $L_{\mu p} = 10^{32} \text{cm}^{-2} \text{s}^{-1}$ was considered in [6]. Also in Ref. [5] the ultimate case of muon beams with 50 TeV energy [2] had been taken into account as an option for 100 TeV CM energy μp colliders assuming that a 50 TeV proton ring would be added into the μC tunnel and a luminosity value $\sim 10^{33} \text{cm}^{-2} \text{s}^{-1}$ is estimated. The FCC based muon-proton and muon-lead ion colliders' main parameter calculations were performed in a recent paper which considers beam-beam effects and a basic collider parameter optimization [7].

In Ref. [8], the physics potentials of μp colliders with several energy and luminosity options (from $\sqrt{s} = 314$ GeV, $L_{\mu p} = 0.1 \text{fb}^{-1}$ per year to $\sqrt{s} = 4899$ GeV,

^{*} This study is supported by TUBITAK under the grant no 114F337.

1) E-mail: ycacar@etu.edu.tr

2) E-mail: ukaya@etu.edu.tr

3) E-mail: b.oner@etu.edu.tr

$L_{\mu p} = 280 fb^{-1}$ per year) were studied. The sensitivity reach of each collider was calculated for some BSM phenomena such as R-parity violating squarks, leptoquarks, leptogluons and extra-dimensions. Similarly, R-parity violating resonances were examined for Tevatron based μp collider with $\sqrt{s} = 0.9$ TeV and $L_{\mu p} = 10^{32} cm^{-2} s^{-1}$ in [9]. In a recent study excited muon production was analyzed at muon-hadron colliders based on the FCC [10].

This paper shows a follow up work of our previous study which was based on the search potential of the FCC-based ep colliders on color octet electrons [11] (besides, there are number of papers devoted to the study of color octet electron production at the LHC [12–15] and LHeC [16–18]).

We now consider another design, namely, the construction of a muon ring tangential to the FCC, which is schematically shown in Fig. 1. The aim is to achieve the highest possible CM energies in lepton-hadron colliders in order to make some of the BSM physics research possible. Here, the physics potential of these future colliders is revealed by quantitatively exploring resonant production of color octet muons. Parameters of the FCC-based muon proton colliders are given in Table I. The first four colliders [7] use the most recent design parameters of MAP [1]. The last row corresponds to the ultimate case with 20 TeV muon beams in the FCC tunnel. 20 TeV choice is due to synchrotron radiation loss of muons which is desired to be limited at 1 GeV/turn for a muon accelerator with 100 km circumference [19].

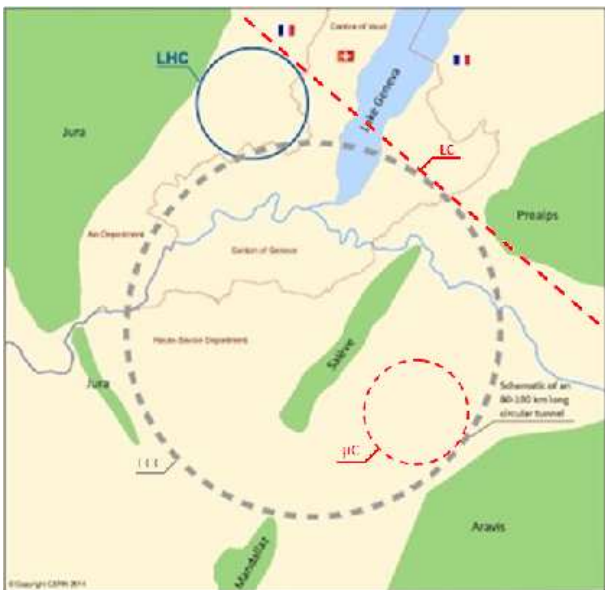


Fig. 1. Possible configuration of the FCC, linear collider (LC) and muon collider (μC).

Table 1. Main parameters of the FCC based μp colliders.

Collider Name	E_μ (TeV)	CM Energy (TeV)	L_{int}, fb^{-1} (per year)
$\mu 63 \otimes FCC$	0.063	3.55	0.02
$\mu 750 \otimes FCC$	0.75	12.2	5
$\mu 1500 \otimes FCC$	1.5	17.3	5
$\mu 3000 \otimes FCC$	3.0	24.5	5
$\mu 20000 \otimes FCC$	20	63.2	10

The rest of the paper is organized as follows. In Section II, we present phenomenology of color octet muon. Section III covers signal-background analyses and is closed by giving the results of discovery limit searches of muon-proton colliders. Section IV addresses the determination of compositeness scales via muon-proton collider options under two possible cases regarding the results of the FCC. Finally, Section V contains summary of the obtained results.

2 Color octet muon

One of the possible answer to the problems mentioned in the Introduction may hide behind the concept of compositeness. Fermion-scalar and three-fermion models are the most proper options which enable known SM leptons to be constructed from more fundamental particles, namely preons. If the SM leptons are composed of color triplet fermions and color triplet scalars, then both fermion-scalar and three-fermion models predict at least one color octet partner to the color singlet leptons:

$$\ell = (F\bar{S}) = 3 \otimes \bar{3} = 1 \oplus 8 \quad (1)$$

$$\ell = (FFF) = 3 \otimes 3 \otimes 3 = 1 \oplus 8 \oplus 8 \oplus 10. \quad (2)$$

Interaction lagrangian of ℓ_s with leptons and gluons can be written as

$$L = \frac{1}{2\Lambda} \sum_l \{ \bar{\ell}_s^\alpha g_s G_{\mu\nu}^\alpha \sigma^{\mu\nu} (\eta_L \ell_L + \eta_R \ell_R) + h.c. \} \quad (3)$$

where g_s is strong coupling constant, Λ denotes compositeness scale, $G_{\mu\nu}$ is gluon field strength tensor, $\ell_{L(R)}$ stands for left (right) spinor components of lepton, $\ell = e, \mu, \tau$; $\sigma^{\mu\nu}$ is the antisymmetric tensor ($\sigma^{\mu\nu} = \frac{i}{2} [\gamma^\mu, \gamma^\nu]$), $\eta_L (\eta_R)$ symbolizes chirality factor. Keeping in mind leptonic chiral invariance ($\eta_L \eta_R = 0$), we take $\eta_L = 1$ and $\eta_R = 0$. Decay width of ℓ_s is given by

$$\Gamma(\ell_s \rightarrow \ell + g) = \frac{\alpha_s M_{\ell_s}^3}{4\Lambda^2} \quad (4)$$

where $\alpha_s = g_s/4\pi$. Dependence of the decay width on the mass of μ_s is presented in Fig. 2 for $\Lambda = M_{\mu_s}$ and $\Lambda = 100$ TeV cases.

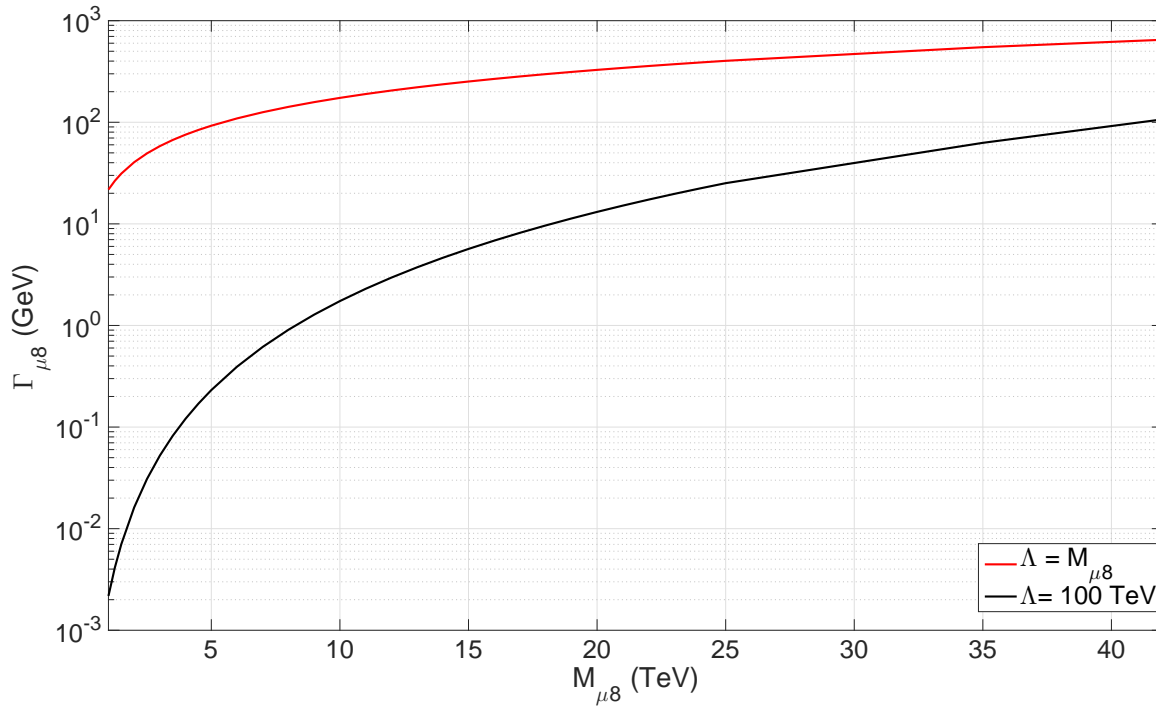


Fig. 2. Color octet muon decay width for $\Lambda = M_{\mu 8}$ and $\Lambda = 100$ TeV.

The resonant μ_8 production (see Figure 3) cross sections for different stages of the FCC based μp colliders from Table I were calculated using MadGraph5 event generator [20]. CTEQ6L1 parametrization [21] was used as parton distribution function and results were presented in Figure 4. MadGraph5-Pythia6 interface was used for parton showering and hadronization [22]. The same tools were used for the rest of the study and further calculations did not take detector effects into account.

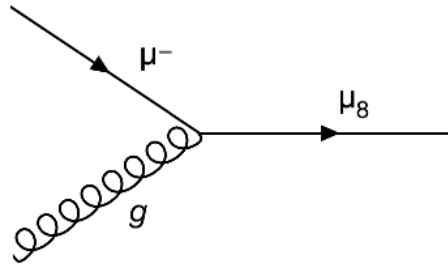


Fig. 3. Feynman diagram for the resonant μ_8 production.

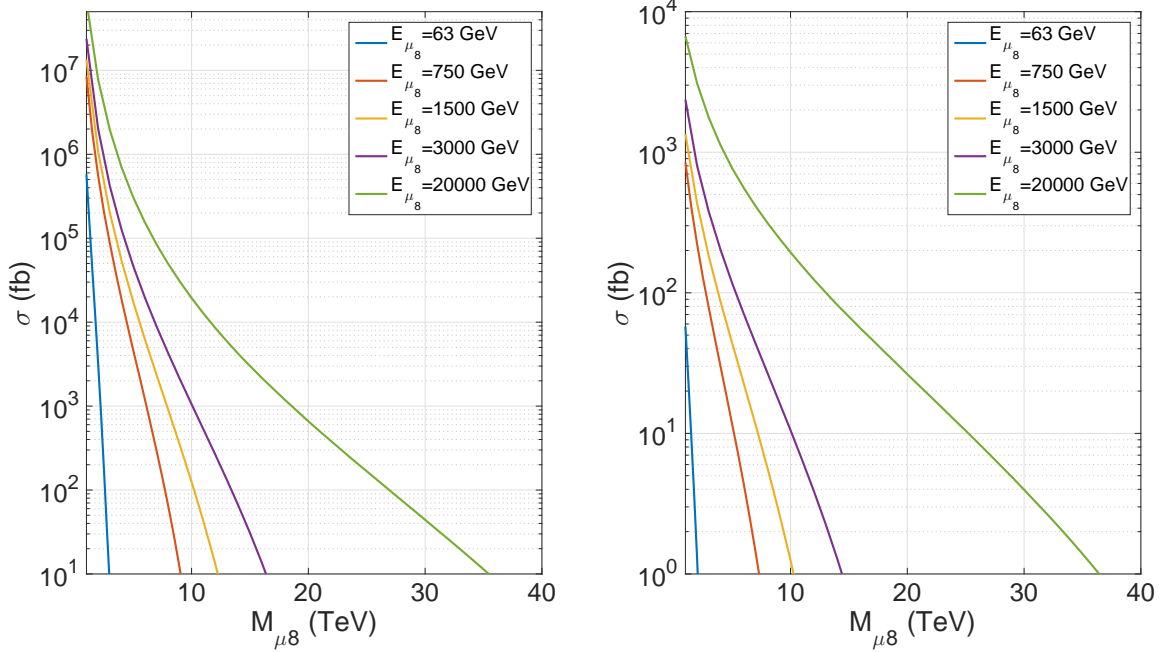


Fig. 4. Resonant color octet muon production at the FCC based μp colliders given in Table I for (a) $\Lambda = M_{\mu_8}$ and for (b) $\Lambda = 100$ TeV ($\mu p \rightarrow \mu_8 X \rightarrow \mu j X$).

3 Signal - Background Analysis

In this section, results of the numerical calculations are shown for the process $p\mu \rightarrow j\mu$ to leading order in order to analyze the search potential of the FCC based muon-proton colliders on the μ_8 discovery via resonant production within $\Lambda = M_{\mu_8}$ scenario. Let us mention that jet corresponds to gluon for signal ($\mu g \rightarrow \mu_8 \rightarrow \mu g$ at partonic level) and quarks for main background ($\mu q \rightarrow \mu q$ through γ and Z exchanges) processes.

A staged approach was applied to determine mass limits as follows. $\mu 63 \otimes \text{FCC}$, the μp collider with minimum CM energy, was chosen as the initial collider where discovery limit of μ_8 mass was to be sought. After the

discovery limit was determined, a worse scenario was considered where μ_8 was assumed to have a larger mass. It was supposed that the previous collider had excluded μ_8 mass up to the corresponding discovery limit and necessary cuts regarding this assumption were applied for the next higher CM energy μp collider. Latter colliders follow the rows of Table I respectively. This procedure ends up with the ultimate μp collider with CM energy 63.2 TeV which was given in the last row of the Table I. One should note that a sequential building of these colliders seems not to be the realistic case. Therefore, if a muon-proton collider is built, color-octet muon search discovery cuts would depend on up-to-date experimental exclusion limits.

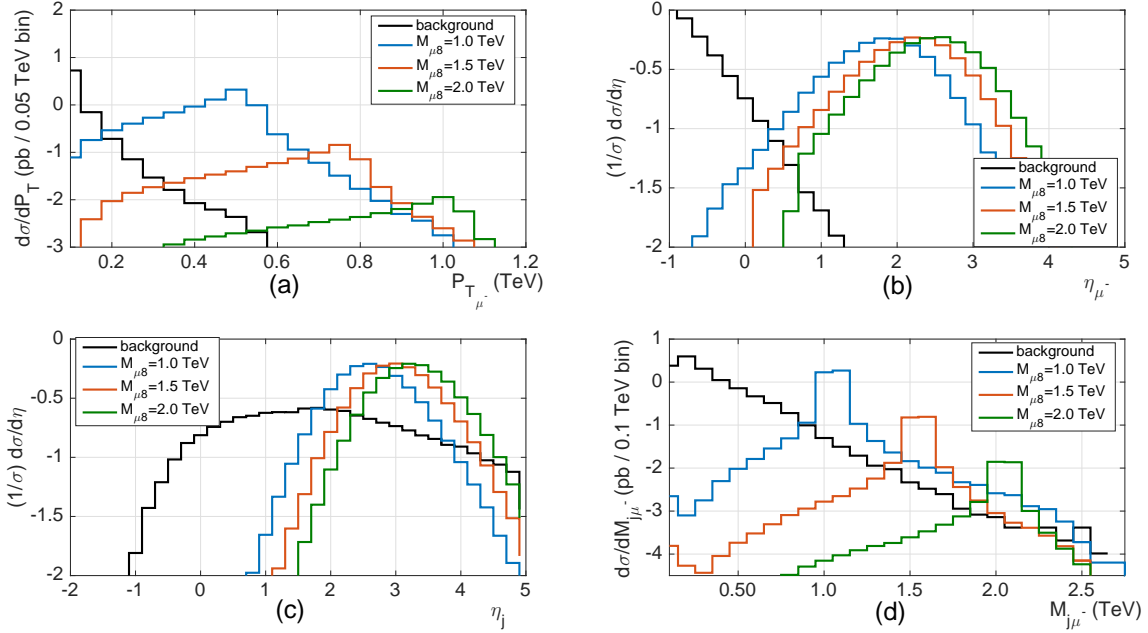


Fig. 5. a) Transverse momentum distributions of final state muons (almost same distribution holds for the leading-jets), b) pseudorapidity distributions of final state muons, c) pseudorapidity distributions of final state jets and d) invariant mass distributions for signal and background at $\mu 63 \otimes \text{FCC}$ after generic cuts.

Kinematical distributions of $\mu 63 \otimes \text{FCC}$ with generic cuts ($p_{T_\mu} > 20$ GeV, $p_{T_j} > 30$ GeV) are given in Fig. 5. Reconsideration of the ATLAS/CMS results in the search for the second generation leptoquarks [23, 24] (which have the same decay channel as μ_8) leads us to the strongest current limit on the color octet muon mass, $M_{\mu_8} \gtrsim 1$ TeV. Therefore, we chose the discovery cut for transverse momentum to be $p_T > 350$ GeV on our initial μp collider. This transverse momentum cut was applied on final state muon as well as leading-jet. In order to suppress the background while keeping the signal cross section as much as possible, the following pseudorapidity cuts were also applied: $2.00 < \eta_j < 4.00$, $0.5 < \eta_\mu < 4.74$. Maximum possible value of η_μ and η_j was taken 4.74 which corresponds to 1° in proton direction. This value can be covered by very forward detector as in the LHeC case [25]. Effects of these discovery cuts can be seen by comparing Fig. 5(d) with Fig. 6 where invariant mass of μ_8 was reconstructed from final state particles μ and leading-jet. After these cuts, cross sections of signals remained almost the same while background cross-section decreased remarkably.

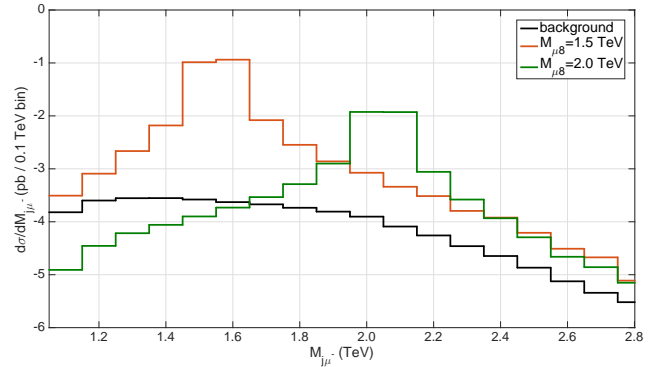


Fig. 6. Invariant mass distributions for signal and background at $\mu 63 \otimes \text{FCC}$ after discovery cuts.

Statistical significance (SS) is calculated using the formula below:

$$SS = \sqrt{2L_{int}} \sqrt{(\sigma_S + \sigma_B) \ln(1 + (\sigma_S/\sigma_B)) - \sigma_S} \quad (5)$$

where σ_S and σ_B denote cross-section values of signal and background, respectively. Integrated luminosity values, L_{int} , of each collider per year was estimated in [7]. Discovery ($SS = 5$) and observation ($SS = 3$) limits for 0.02 fb^{-1} $\mu 63 \otimes \text{FCC}$ integrated luminosity were found to be 2380 and 2460 GeV, respectively. Regarding these results of the minimum energy μp collider, $p_T > 800$ GeV was considered appropriate for the next stage $\mu 750 \otimes \text{FCC}$

Table 2. Kinematical discovery cuts and observation (3σ) and discovery (5σ) limits for μ_8 at different μp colliders. Transverse momentum cuts are given in TeV. Significance values are calculated locally.

Collider Name	L_{int}, fb^{-1}	Kinematical Cuts					$M_{\mu_8} \pm PDF\% \pm scale\%$, TeV					
		$p_{T_{min}}$	$\eta_{\mu_{min}}$	$\eta_{\mu_{max}}$	$\eta_{j_{min}}$	$\eta_{j_{max}}$	3σ		5σ			
$\mu 63 \otimes FCC$	0.02	0.350	0.5	4.74	2.0	4.0	2.46	+2.60% +1.63%	-1.83% -1.75%	2.38	+2.52% +1.68%	-2.10% -1.89%
$\mu 750 \otimes FCC$	5	0.800	-1.3	4.74	1.0	4.1	9.60	+1.34% +0.63%	-1.15% -1.27%	9.21	+1.46% +0.74%	-1.20% -1.37%
$\mu 1500 \otimes FCC$	5	3.00	-1.7	4.74	0.7	3.9	13.8	+1.30% +0.51%	-1.01% -0.87%	13.2	+1.36% +0.53%	-1.14% -1.06%
$\mu 3000 \otimes FCC$	5	4.40	-2.1	4.74	0.3	3.5	18.9	+1.22% +0.53%	+1.27% +0.44%	18.1	-1.01% -0.63%	-1.22% -0.77%
$\mu 20000 \otimes FCC$	10	6.00	-2.7	4.74	-0.7	2.7	42.7	+1.57% +0.59%	-1.29% -0.58%	41.5	+1.61% +0.63%	-1.40% -0.60%

and similar analyses were performed. These consecutive calculations gave us mass reach of each collider as given in Table II. Applied discovery cuts were also given in the same table and mass window formulation was kept same for all calculations: $M_{\mu_8} - 2\Gamma_{\mu_8} < M_{\mu_8} < M_{\mu_8} + 2\Gamma_{\mu_8}$.

Signal and background event numbers were calculated directly in this mass window without using any binning algorithm. Invariant mass distributions after discovery cuts related to higher energy colliders are presented in Figure 7.

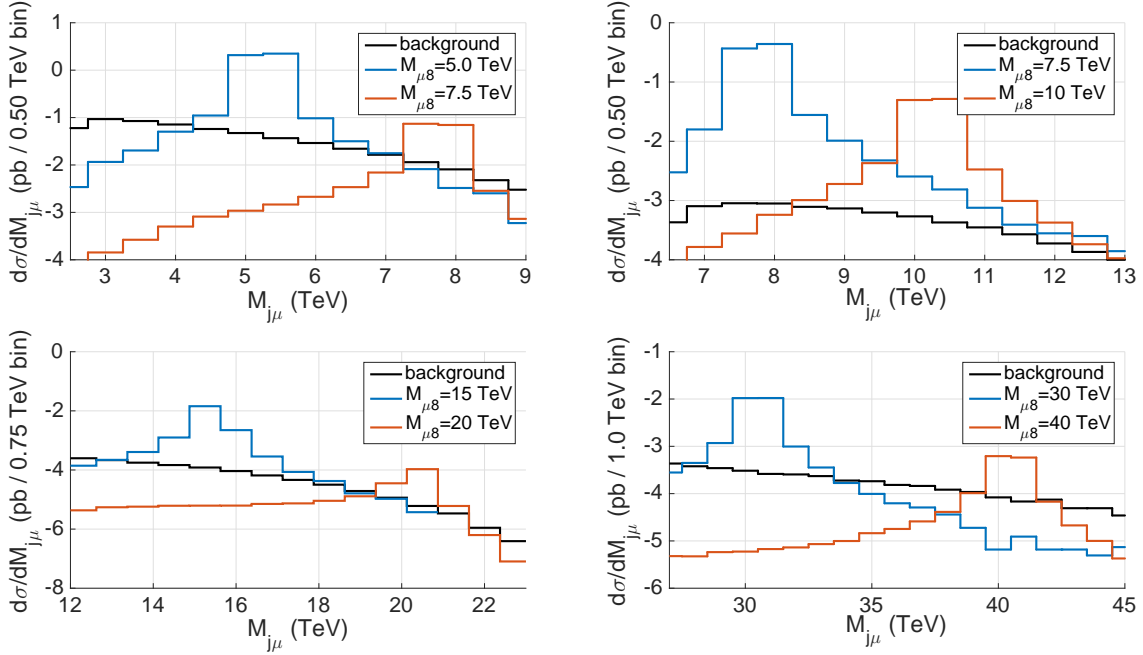


Fig. 7. Invariant mass distributions for signal and background at a) $\mu 750 \otimes FCC$, b) $\mu 1500 \otimes FCC$, c) $\mu 3000 \otimes FCC$ and for d) the ultimate case $\mu 20000 \otimes FCC$ colliders after discovery cuts.

4 Limits on compositeness scale

If the μ_8 is discovered by the FCC-pp option, μp colliders will give opportunity to estimate compositeness scale. In this regard, two distinct possibilities should be considered:

a) μ_8 is discovered by the FCC but not observed at μ -FCC. In this case one can put lower limit on compositeness scale,

b) μ_8 is discovered by the FCC and also observed at μ -FCC. In this case one can determine compositeness scale.

In this section we present the analysis of these two possibilities for four different benchmark points, namely, $M_{\mu_8} = 2.5, 5, 7.5$ and 10 TeV.

4.1 μ_8 is discovered by the FCC but not observed at μ -FCC

If we assume that μ_8 mass is found out by FCC results then it is possible to determine optimal cuts for given M_{μ_8} at the μ -FCC colliders. Let us start by consideration of $M_{\mu_8} = 5.0$ TeV at $\mu 750 \otimes \text{FCC}$.

It is seen from Fig. 8 that $-1.3 < \eta_\mu < 4.74$ and $0.7 < \eta_j < 3.3$ cuts drastically decrease the background whereas the signal is slightly affected. Similar cuts were determined for other μ -FCC collider options and M_{μ_8} values and these optimal cuts were presented in Table III. Invariant mass window $0.99M_{\mu_8} < M_{j\mu} < 1.01M_{\mu_8}$ has been used in this particular analysis. $\mu 63 \otimes \text{FCC}$ collider was not included in this section due to its remarkably low potential compared to the other options.

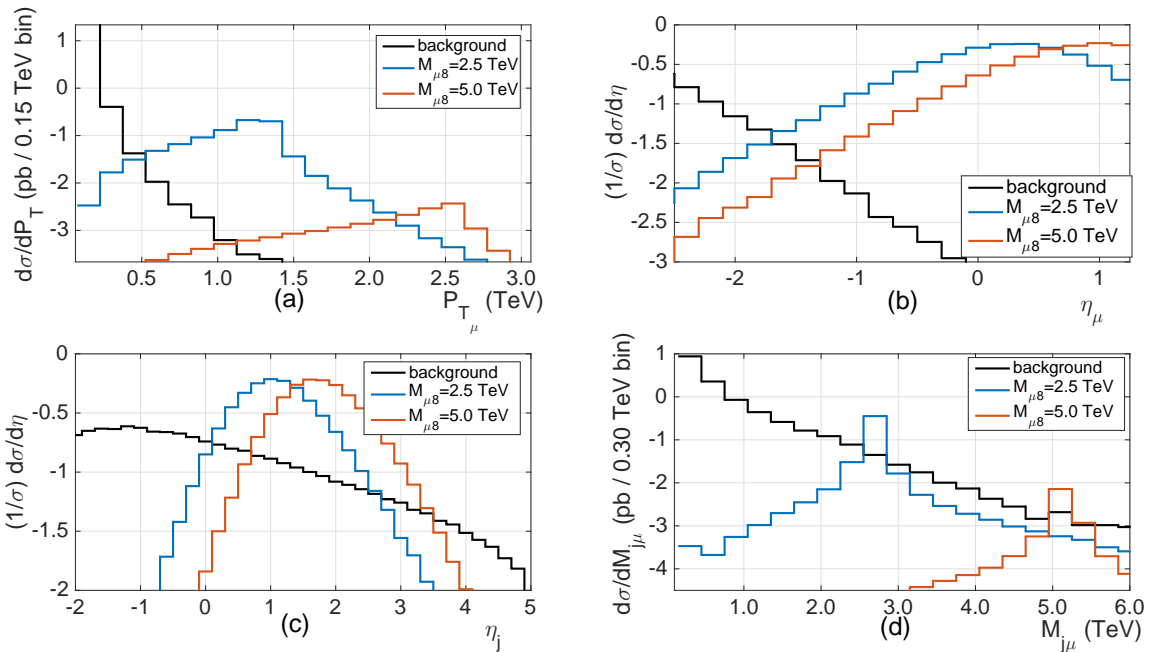


Fig. 8. a) Transverse momentum distributions of final state muons (almost same distribution holds for the leading-jets), b) pseudorapidity distributions of final state muons, c) pseudorapidity distributions of final state jets and d) invariant mass distributions for signal and background at $\mu 750 \otimes \text{FCC}$ after generic cuts.

Applying cuts presented in Table III and $p_T > 350$ GeV for all cases one can estimate achievable lower limits on compositeness scale. Using Eq. 5 we obtain Λ values given in Table IV. As expected, lower bounds on compositeness scale is decreased with increasing value of

the μ_8 mass. It is seen that multi-hundred TeV lower bounds can be put on the compositeness scale if μ_8 is discovered at the FCC and not observed at any $\mu \otimes \text{FCC}$.

Table 3. Optimal cuts for determination of compositeness scale lower bounds.

Collider	Cut Type	$M_{\mu_s} = 2.5$ TeV		$M_{\mu_s} = 5.0$ TeV		$M_{\mu_s} = 7.5$ TeV		$M_{\mu_s} = 10$ TeV	
		min	max	min	max	min	max	min	max
$\mu 750 \otimes \text{FCC}$	η_μ	-1.7	4.74	-1.3	4.74	-1.2	4.74	-	-
	η_j	0.2	2.6	0.7	3.3	1.0	3.9	-	-
	Mass Window (GeV)	2475	2525	4950	5050	7425	7575	-	-
$\mu 1500 \otimes \text{FCC}$	η_μ	-2.3	4.74	-2.0	4.74	-1.8	4.74	-1.7	4.74
	η_j	-0.6	1.9	-0.1	2.7	0.4	3.1	0.5	3.5
	Mass Window (GeV)	2475	2525	4950	5050	7425	7575	9900	10100
$\mu 3000 \otimes \text{FCC}$	η_μ	-2.9	4.74	-2.7	4.74	-2.5	4.74	-2.3	4.74
	η_j	-1.4	1.4	-0.8	2.1	-0.4	2.6	-0.2	3.1
	Mass Window (GeV)	2475	2525	4950	5050	7425	7575	9900	10100
$\mu 20000 \otimes \text{FCC}$	η_μ	-3.9	4.74	-3.5	4.74	-3.3	4.74	-3.2	4.74
	η_j	-3.0	-0.9	-2.5	0.1	-2.1	0.5	-1.9	1.0
	Mass Window (GeV)	2475	2525	4950	5050	7425	7575	9900	10100

Table 4. Lower limits on compositeness scale in TeV units at the FCC based μp colliders.

Collider	L_{int}, fb^{-1}	$M_{\mu_s} = 2.5$ TeV		$M_{\mu_s} = 5.0$ TeV		$M_{\mu_s} = 7.5$ TeV		$M_{\mu_s} = 10$ TeV	
		3σ	5σ	3σ	5σ	3σ	5σ	3σ	5σ
$\mu 750 \otimes \text{FCC}$	5	270	210	170	130	50	35	-	-
$\mu 1500 \otimes \text{FCC}$	5	360	280	220	170	130	100	55	40
$\mu 3000 \otimes \text{FCC}$	5	475	370	320	245	230	170	140	105
$\mu 20000 \otimes \text{FCC}$	10	1390	1080	850	655	515	400	315	246

4.2 μ_8 is discovered by the FCC and observed at μ -FCC

In this case, the value of cross section at μp colliders, which is inversely proportional to Λ^2 gives the opportunity to determine the compositeness scale directly. As an

example, let us consider the $\mu 1500 \otimes \text{FCC}$ case. In Fig. 9 we present Λ dependence of μ_8 production cross section for $M_{\mu_8} = 2.5, 5, 7.5$ TeV. Supposing that FCC discovers μ_8 with 5 TeV mass and $\mu 1500$ -FCC measures cross section as $\sigma_{exp} \sim 100$ fb, one can derive the compositeness scale as $\Lambda_{exp} \simeq 70$ TeV.

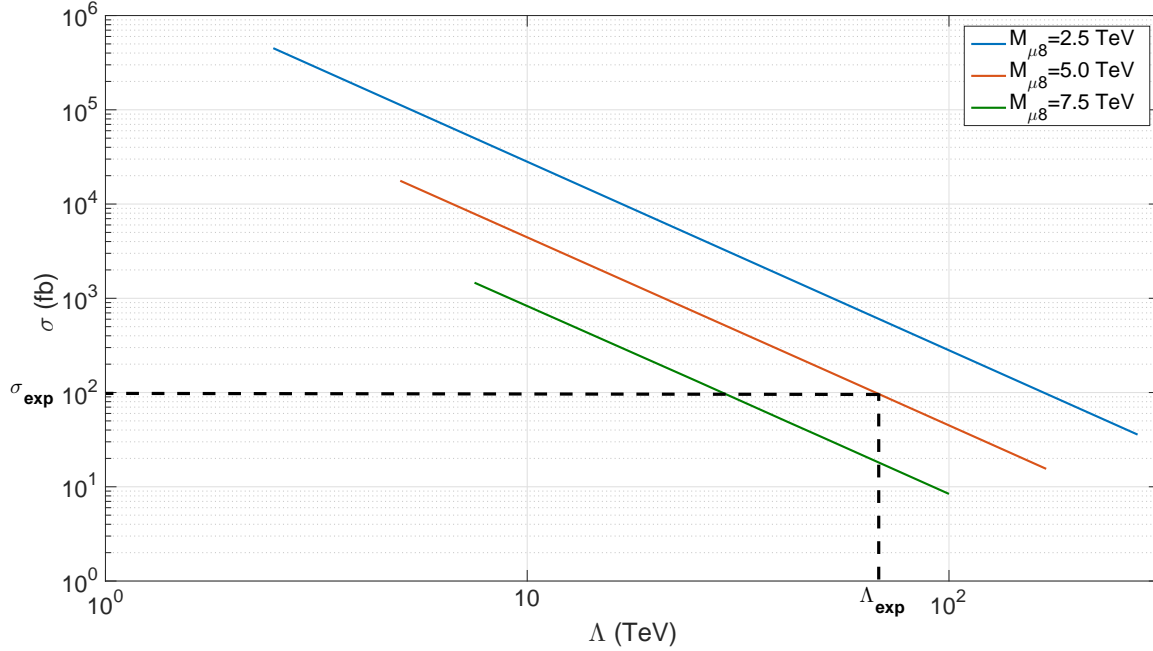


Fig. 9. Cross section distributions with respect to compositeness scale for $\mu 1500 \otimes \text{FCC}$ collider.

4.3 μ_8 is not discovered by FCC but observed at μ -FCC

Another possibility is the failure of μ_8 search at the FCC. This can be caused by the value of color-octet muon mass, M_{μ_8} , which can be greater than the discovery limit of the FCC itself. In this case, the advantages of μ -FCC colliders with quite large discovery limits manifest themselves.

5 Conclusion

Discovery mass limits for μ_8 at the muon, proton and FCC based μp colliders are shown in Fig. 10. It is obvious that discovery mass limits for pair production of μ_8 at muon colliders are approximately half of CM energies.

Discovery limit values for LHC and FCC are obtained by rescaling ATLAS/CMS second generation LQ results [23, 24] using the method developed by G. Salam and A. Weiler [26]. Following [27], integrated luminosity values 3 ab^{-1} and 20 ab^{-1} have been used for the High Luminosity LHC (HL-LHC) and the FCC-hh, respectively. As can be seen from Fig. 10, FCC based μp colliders with a discovery limit up to 40 TeV are the most advantageous among the other collider options for μ_8 searches. Moreover, FCC based μp colliders will give the opportunity to probe compositeness up to the PeV scale.

The authors are grateful to Saleh Sultansoy for useful discussions. The authors are also grateful to Subhadip Mitra and Tanumoy Mandal for sharing their leptogluon MadGraph model file. This paper is to be published in Chinese Physics C.

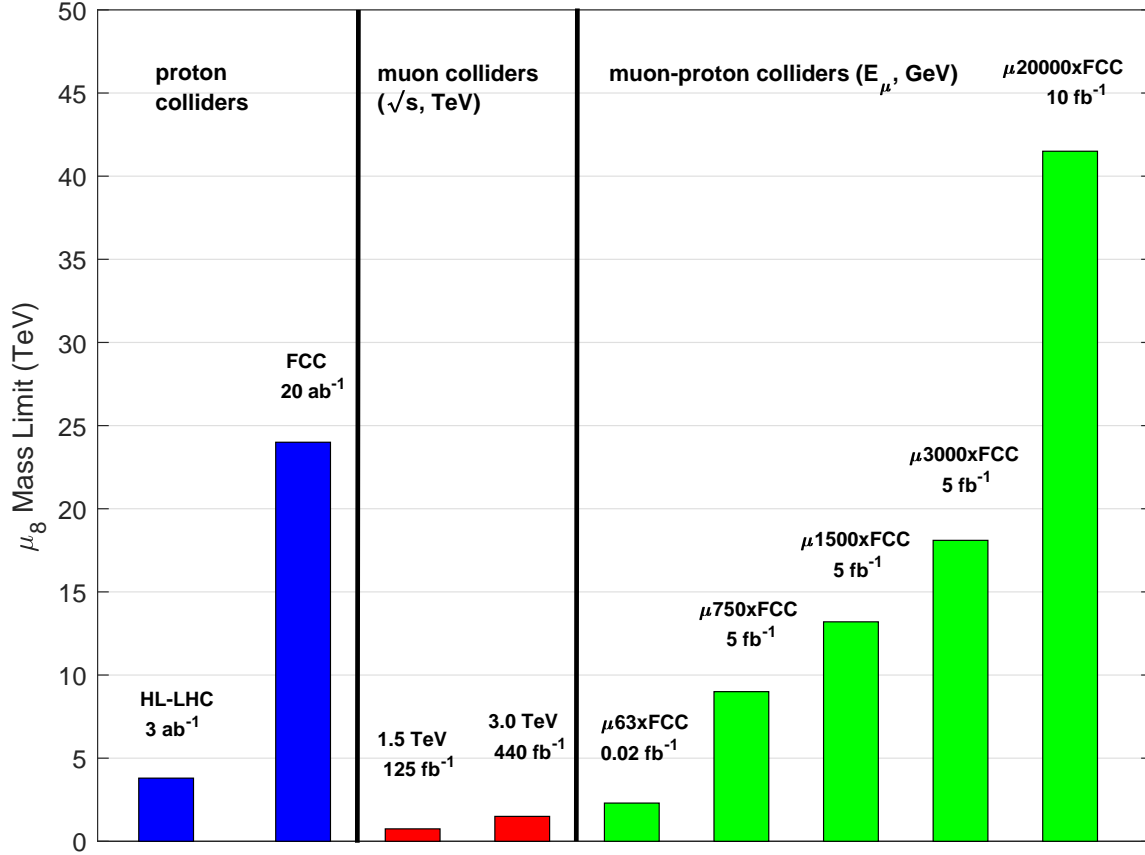


Fig. 10. Mass discovery limits ($SS = 5$) of the color octet muon regarding different type of colliders, i.e. proton, muon and muon-proton.

References

- J. P. Delahaye et al, Enabling intensity and energy frontier science with a muon accelerator facility in the U.S., arXiv:1308.0494v2 [physics.acc-ph].
- B.J. King, Parameter Sets for 10 TeV and 100 TeV Muon Colliders, and their Study at the HEMC'99 Workshop, arXiv:physics/0005008 [physics.acc-ph].
- FCC web page: <https://fcc.web.cern.ch>.
- I.F. Ginzburg, Physics at future e p, gamma p (linac-ring) and mu p colliders, Turk J. Phys 22, 607 (1998).
- S. Sultansoy, "The post-HERA era: brief review of future lepton-hadron and photon-hadron colliders", DESY 99-159, arXiv:hep-ph/9911417v2.
- V.D. Shiltsev, "An asymmetric muon proton collider: luminosity consideration", in Proceedings of 1997 Particle Accelerator Conference, 1998 (Vancouver, British Columbia, Canada), p. 420.
- Y.C. Acar *et al.*, "FCC Based Lepton-Hadron and Photon-Hadron Colliders: Luminosity and Physics", arXiv:1608.02190 [physics.acc-ph].
- K. Cheung, "Muon-proton colliders: Leptoquarks, contact interactions and extra dimensions", AIP Conference Proceedings 542 (2000) 160.
- M. Carena, D. Choudhury, C. Quigg, S. Raychaudhuri, Study of R-parity violation at a μp collider, Phys. Rev. D 62(9) (2000), arXiv: 095010.
- A. Caliskan, S.O. Kara, A. Ozansoy, "Excited muon searches at the FCC based muon-hadron colliders", arXiv:1701.03426 [hep-ph].
- Y.C. Acar, U. Kaya, B.B. Oner, and S. Sultansoy, "Color octet electron search potential of the FCC based e-p colliders", arXiv:1605.08028v2 [hep-ph].
- A. Celikel, M. Kantar, S. Sultansoy, "A search for sextet quarks and leptogluons at the LHC", Phys. Lett. B. 443(1) (1998).
- T. Mandal and S. Mitra, "Probing color octet electrons at the LHC", Phys. Rev. D., 87(9) (2013), arXiv:1211.6394v2 [hep-ph].
- D. Gonalves-Netto, D. Lopez-Val, K. Mawatari, I. Wigmore, T. Plehn, "Looking for leptogluons", Phys. Rev. D., 87(9) (2013), arXiv:1303.0845v1 [hep-ph].
- T. Mandal, S. Mitra, S. Seth, "Probing compositeness with the CMS $e e j j$ & $e e j$ data", Phys. Lett. B. 758 (2016), arXiv:1602.01273v2 [hep-ph].
- A. Celikel and M. Kantar, "Resonance Production of New Resonances at ep and γp Colliders", Tr. J. of Physics 22 (1998)

-
- 401.
- 17 M. Sahin, S. Sultansoy and S. Turkoz, “Resonant production of color octet electron at the LHeC”, Phys. Lett. B 689 (2010) 172.
- 18 M. Sahin, “Resonant production of spin-3/2 color octet electron at the LHeC”, Acta Physica Polonica B 45 (2014) 1811.
- 19 S. Sultansoy talk at 1st FCC Physics Workshop (CERN), <https://indico.cern.ch/event/550509/contributions/2413830>.
- 20 J. Alwall *et al.*, “The automated computation of tree-level and next-to-leading order differential cross sections, and their matching to parton shower simulations”, JHEP 2014(7) (2014); arXiv:1405.0301v2 [hep-ph].
- 21 D. Stump *et al.*, “Inclusive jet production, parton distributions and the search for new physics”, JHEP 0310 (2003) 046.
- 22 T. Sjostrand, S. Mrenna, and P.Z. Skands, “PYTHIA 6.4 physics and manual,” JHEP 0605 (2006) 026, arXiv:hep-ph/0603175 [hep-ph].
- 23 V. Khachatryan *et al.* (CMS Collaboration), “Search for pair production of first and second generation leptoquarks in proton-proton collisions at $\sqrt{s}= 8$ TeV”, Phys. Rev. D 93, (2016) 032004.
- 24 ATLAS Collaboration, “Search for scalar leptoquarks in pp collisions at $\sqrt{s}=13$ TeV with the ATLAS experiment”, arXiv:1605.06035v2 [hep-ex].
- 25 J.L. Abelleira Fernandez *et al.* (LHeC Study Group), “A Large Hadron Electron Collider at CERN: Report on the Physics and Design Concepts for Machine and Detector”, J. Phys. G: Nucl. Part. Phys. 39, (2012) 075001.
- 26 G. Salam and A. Weiler, “The Collider Reach project”, <http://collider-reach.web.cern.ch/collider-reach>.
- 27 M. Benedikt, X. Buffat, D. Schulte, F. Zimmermann, “Luminosity targets for FCC-hh ”, in Proceedings of 2016 International Particle Accelerator Conference (Busan, Korea), p.1523.